Experimental Study on Merits of Virtual Cleaning of Paintings with Aged Varnish

Trumpy, Giorgio

DOI: https://doi.org/10.1364/OE.23.033836

Experimental study on merits of virtual cleaning of paintings with aged varnish

Giorgio Trumpy,[1] Damon Conover,[1,2] Lionel Simonot,[3] Mathieu Thoury,[1] Marcello Picollo[4] and John K. Delaney[1,2,*]

[1]*Scientific Research Department, National Gallery of Art, Constitution Avenue, NW, Washington, D.C. 20565, USA*
[2]*George Washington University, 2121 I Street, NW, Washington, D.C. 20052, USA*
[3]*Institut Pprime, CNRS UPR 3346, University of Poitiers, SP2MI, Boulevard Marie et Pierre Curie 86962 Futuroscope-Chasseneuil, France*
[4]*Institute of Applied Physics "N. Carrara", Via Madonna del Piano 10, 50019 Sesto Fiorentino, Italy*

[*]*J-Delaney@NGA.GOV*

Abstract: To assess the accuracy of *virtual cleaning* of Old Master paintings (i.e. digital removal of discolored varnishes), a physical model was developed and experimentally tested using reflectance imaging spectroscopy on three paintings undergoing conservation treatment. The model predicts the reflectance spectra of the painting without varnish or after application of a new varnish from the reflectances of the painting with the aged varnish, given the absorption of the aged varnish and the scattering terms. The resulting color differences between the painting actually and virtually cleaned can approach the perceivable limit. Residual discrepancies are ascribable to spatial variations in the characteristics of the aged varnish (scattering, optical thickness) and the exposed painting (surface roughness).

OCIS codes: (110.4234) Multispectral and hyperspectral imaging; (100.3020) Image reconstruction-restoration; (240.5770) Roughness; (330.1710) Color, measurement.

References and links

1. P. Cotte and D. Dupraz, "Spectral imaging of Leonardo Da Vinci's Mona Lisa: A true color smile without the influence of aged varnish," in *3rd European Conference on Colour in Graphics, Imaging, and Vision* (IS&T, 2006), pp. 311–317.
2. G. Schirripa Spagnolo, "Virtual restoration: detection and removal of craquelure in digitized image of old paintings," Proc. SPIE **8084**, O3A: Optics for Arts, Architecture, and Archaeology III, 80840B (2011).
3. R. S. Berns, Rejuvenating the Appearance of Cultural Heritage Using Color and Imaging Science Techniques, in *Proceedings of the 10th Congress of the International Colour Association,* J. L. Nieves and J. Hernández-Andrés, ed. (AIC, 2005), pp. 369–374.
4. G. M. Cortelazzo, G. L. Geremia, and G. A. Mian, "Some results about Wiener-Volterra restoration of the original colour quality in old painting imagery," in *Proceedings of IEEE Workshop Nonlinear Signal Image Processing* (NSIP, 1995), pp. 86–89.
5. M. Pappas and I. Pitas, "Digital color restoration of old paintings," IEEE Trans. Image Process. **9**(2), 291–294 (2000).
6. M. Barni, F. Bartolini, and V. Cappellini, "Image processing for virtual restoration of artworks," IEEE Multimedia Mag. **7**(2), 34–37 (2000).
7. CIE, "CIE Colorimetry - Part 1: Standard Colorimetric Observers," ISO 11664-1:2007(E)/CIE S 014-1/E:2006.
8. P. Urban and R. R. Grigat, "Metamer density estimated color correction," Signal Image Video Process. **3**(171), 171–182 (2009).
9. K. Martinez, J. Cupitt, and D. Saunders, "High-resolution colorimetric imaging of paintings," Proc. SPIE **1901**, 25 (1993).

#253141 Received 5 Nov 2015; revised 13 Dec 2015; accepted 14 Dec 2015; published 23 Dec 2015

10. S. Baronti, A. Casini, F. Lotti, and S. Porcinai, "Multispectral imaging system for the mapping of pigments in works of art by use of principal-component analysis," Appl. Opt. **37**(8), 1299–1309 (1998).
11. F. H. Imai and R. S. Berns, "High-resolution multi-spectral image capture for fine arts preservation," in *Proc. 4th Argentina Color Conference* (1998), pp. 21–22.
12. A. Casini, M. Bacci, C. Cucci, F. Lotti, S. Porcinai, M. Picollo, B. Radicati, M. Poggesi, and L. Stefani, "Fiber optic reflectance spectroscopy and hyper-spectral image spectroscopy: two integrated techniques for the study of the Madonna dei Fusi," Proc. SPIE **5857**, Optical Methods for Arts and Archaeology, 58570M (2005).
13. J. K. Delaney, J. G. Zeibel, M. Thoury, R. Littleton, M. Palmer, K. M. Morales, E. R. de la Rie, and A. Hoenigswald, "Visible and Infrared Imaging Spectroscopy of Picasso's Harlequin Musician: Mapping and Identification of Artist Materials in Situ," Appl. Spectrosc. **64**(6), 584–594 (2010).
14. T. B. Brill, *Light: Its Interaction with Art and Antiquities* (Plenum, 1980).
15. E. R. de la Rie, "The influence of varnishes on the appearance of paintings," Stud. Conserv. **32**(1), 1–13 (1987).
16. E. R. de la Rie, J. K. Delaney, K. M. Morales, C. A. Maines, and L. P. Sung, "Modification of Surface Roughness by Various Varnishes and Effect on Light Reflection," Stud. Conserv. **55**(2), 134–143 (2010).
17. E. R. de la Rie, "Degradation and Stabilization of Varnishes for Paintings," in *Preprints to the 13th International Conference in the Stabilization and Degradation of Polymers* (1991), pp. 129–139.
18. C. M. Palomero and M. Soriano, "Digital cleaning and 'dirt' layer visualization of an oil painting," Opt. Express **19**(21), 21011–21017 (2011).
19. M. Bacci, A. Casini, C. Cucci, M. Picollo, B. Radicati, and M. Vervat, "Non-invasive spectroscopic measurements on the Il ritratto della figliastra by Giovanni Fattori: identification of pigments and colourimetric analysis," J. Cult. Herit. **4**, 329–336 (2003).
20. J. Kirby, D. Saunders, and J. Cupitt, "Colorants and Colour Change," in *Early Italian Painting Techniques and Analysis,* T. Bakkenis, R. Hoppenbrouwers, H. Dubois, ed. (Limburg Conservation Institute, 2005), pp. 60–66.
21. D. M. Conover, J. K. Delaney, and M. H. Loew, "Automatic registration and mosaicking of technical images of Old Master paintings," Appl. Phys. A **119**(4), 1567–1575 (2015).
22. S. A. Shafer, "Using color to separate reflection components," Color Res. Appl. **10**(4), 210–218 (1985).
23. R. S. Hunter, *The Measurement of Appearance* (J. Wiley & Sons, 1975).
24. P. Kubelka, "New contributions to the optics of intensely light-scattering material - part I," J. Opt. Soc. Am. **38**, 448–457 (1948).
25. J. H. Nobbs, "Kubelka-Munk theory and the prediction of reflectance," Rev. Prog. Coloration **15**, 66–75 (1985).
26. R. L. Herbert, *Georges Seurat, 1859–1891* (The Metropolitan Museum of Art, 1991), p. 405.
27. CIE, "CIE Colorimetry - Part 4: 1976 L*a*b* Colour Space," ISO 11664-4:2008(E)/CIE S 014-4/E:2007.

1. Introduction

1.1. Accurate color images of fine art and 'virtual restoration'

In the 1990s photography departments at museums abandoned the use of color film and switched to digital color cameras to capture images of artworks in their collections. The ease of manipulating the digital numbers of the Red, Green and Blue channels over the concentration of color dyes in photographic film (cyan, magenta and yellow dyes) allowed for better accuracy, and a path to 'perfect color reproductions'. Images with more accurate colors gave conservators the ability to follow changes in the appearance of paintings during conservation treatments (e.g. removal of discolored varnish and prior inpainting, new inpainting and new varnishing).

Another opportunity offered by digital imaging is the ability to simulate how a painting would look without the effects of degradation (*virtual restoration*). Different methodologies have been proposed to attempt virtual restoration for diverse types of degradation. The virtual removal of the discolored varnish on Leonardo's "Mona Lisa" was attempted [1] and other types of degradation were tackled, such as the *craquelure* [2] and fading of the eosin dye (geranium lake) [3] that affects many of Van Gogh's paintings. Early studies on virtual restoration [4–6] were working with tri-dimensional color spaces. Unfortunately, the color accuracy of trichromatic cameras has limitations, which are a consequence of the differences in the spectral response of cameras compared to the human visual system (i.e. the CIE standard observer [7]). Thus, color pairs discernible by the human visual system can result in the same RGB value, or conversely, the camera can register different RGB values for a color pair indistinguishable for the human eye (*metamer mismatch*) [8]. In view of this, increasing the number of spectral channels from three to five or more has been shown to reduce metamer mismatch [9–11].

#253141 Received 5 Nov 2015; revised 13 Dec 2015; accepted 14 Dec 2015; published 23 Dec 2015

In recent years calibrated hyperspectral cameras (spectral sampling < 5 nm) have provided diffuse reflectance spectra of polychrome surfaces even at high spatial resolution [12,13]. While this degree of spectral sampling is more than what is required for determining color coordinates, it offers the opportunity to identify pigments in a non-destructive way, and at the same time it allows the precise study of the optical effects associated with pigment fading and varnish discoloration. Accurate diffuse reflectance spectra, coupled with a physical model that precisely describes the optical phenomena at the paint surface, would provide a complete system to explore the effectiveness of virtual restoration.

1.2. The effect of varnish and its degradation

Paintings are varnished to increase gloss and color saturation, especially in the dark passages. Varnishes and resins are thin transparent layers tens of micrometers thick, with a refractive index similar to the binding medium (see Fig. 1). Research has shown that increased gloss is achieved by creating a new surface (the air/varnish interface) having a smaller roughness (RMS roughness < 0.1 μm) than the paint surface [14, 15]. Varnishes with low molecular weight, such as natural mastic and dammar or the synthetic resin Regalrez®, produce smooth surfaces eliminating both high- and low-spatial frequency roughness [16].

The aging of varnishes is known to decrease the lightness of white and blue areas due to the discoloration and to make the dark areas look lighter, thus decreasing the overall dynamic range. In fact, natural varnishes degrade with time as a result of radical driven oxidation reactions; these reactions are activated by UV/blue light and heat [17]. The products of these reactions absorb the short wavelengths of the visible range (cause of the typical yellowing) and the loss of optical homogeneity due to micro-cracks induces scattering (Fig. 1 - left). The transparency of varnish can also be affected by the accumulation of grime (e.g. candle soot, grease, etc.).

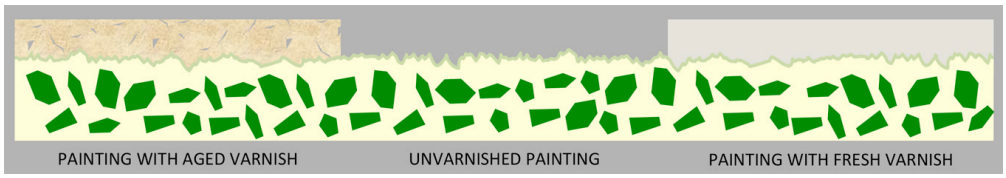

Fig. 1. Diagram illustrating a cross-section of a painting (the substrate of pigment/binder matrix) covered by semi-transparent layer of degraded varnish (left), uncovered (center) and covered by a fresh transparent varnish (right).

1.3. Virtual cleaning, i.e. virtual removal of aged and discolored varnishes

Physical varnish removal can be a lengthy conservation treatment using mild solvents and gels systems. The optical simulation of the result of removing an aged varnish and grime from a painting is known as *virtual cleaning*. An effective virtual cleaning can provide to conservators and curators the change in appearance that would likely occur if the cleaning was undertaken. The simulation gains even more importance in cases where the painting is unlikely to undergo varnish removal in the near future, such as the 'Mona Lisa' by Leonardo da Vinci, whose virtually restored image would be of interest not only to conservators but also the public.

In a recent study [18] a neural network was trained to learn the color transformation between degraded parts of a painting and parts that did not degrade since they were protected by the frame. In a second part of this study, after estimating the reflectance spectra of the painting from the color data, the authors considered the aged varnish ('dirt layer') as a colored filter that can be virtually removed by nullifying its absorption. The exploitation of protected parts of paintings

#253141 Received 5 Nov 2015; revised 13 Dec 2015; accepted 14 Dec 2015; published 23 Dec 2015

to infer the original appearance was already attempted some years before [19,20]. In the virtual cleaning of the 'Mona Lisa' [1] the varnish absorption was measured on mock-up paints glazed with an artificially aged varnish. Since the painting did not undergo varnish removal, the validity of the results cannot be assessed. These studies in general lacked a complete physical model for the varnish/painting system.

The aim of the present study is to directly test the limits of virtual cleaning by measuring the changes in diffuse reflectance of Old Master paintings undergoing actual varnish removal. The study provides a better understanding of the optical impact of aged varnishes on the appearance of paintings by developing a physical model. Three paintings from the collection of the National Gallery of Art in Washington DC were analyzed. A preliminary study was conducted on a still life painted by Willem Kalf (64.5 $\times$ 54 cm). Thereafter two panel paintings were followed during their conservation treatment: a small (15.5 $\times$ 25 cm) impressionist panel by Georges Seurat entitled "Haymakers at Montfermeil", and a Dutch still life (80 $\times$ 60 cm) by Jan van Huysum entitled "Flowers in an urn".

2. Experimental measurements

The experimental method used here was to measure the diffuse reflectance spectra of paintings before and after the removal of aged varnishes, as well as after application of a fresh varnish. The removed varnish was solubilized and its absorbance in solution was measured. Two types of reflectance measurements were performed: point-based Fiber Optics Reflectance Spectroscopy (FORS) and hyperspectral diffuse reflectance imaging spectroscopy (RIS). The FORS spectra, which have an extended spectral range, have been useful to study the optical phenomena associated with aged varnishes extending in the near infrared (from 1000 to 2500 nm) (Section 3). RIS allowed creating the final image product of virtual cleaning, i.e. the color accurate image of the clean painting predicted by the model (Section 7).

FORS spectra were collected with a spectroradiometer (FS3, ASD Inc. - Boulder, CO) [13] that operated from 350 nm to 2500 nm, with a spectral sampling of 1.4 nm from 350 to 1000 nm and 2 nm from 1000 to 2500 nm. The measurements were carried out in a 45/0 geometry, collecting the reflected light at 0° with a 1 mm fiber having a divergence half-angle of 0.11 rad, resulting in a measured area at the painting $\simeq$1 cm$\varnothing$.

RIS hyperspectral images (*cubes*) were collected with a whiskbroom scanning system operating in the visible and infrared range from 400 to 950 nm with a spectral sampling of 2.5 nm. The system used a modified hyperspectral camera (730 Surface Optics, CA) in which the standard focal plane was replaced by a back-side illuminated 1024 by 1024 pixel Si EMCCD array (ProEM: 1024B, Princeton Instruments - Trenton, NJ), operating at -60°C to increase the sensitivity. Illumination was provided by six 50 W, 4700 K lamps (Solux - Rochester, NY) at 45° from the painting normal, producing an illuminance at the paintings surface of 1400 lux, and the integration time was 100 msec per line. For the small impressionist panel the projected pixel size was 0.23 mm, which were acquired with a scan speed of 0.69 mm/sec and a frame rate of 3 Hz. For the Dutch still life the pixel size was 0.44 mm, which were acquired with a scan speed of 1.32 mm/sec and a frame rate of 3 Hz. The calculation of apparent reflectance was done using a white diffuse reflectance standard (25 by 25 cm 98%, Spectralon); further calibration was done with the 'empirical line correction' in ENVI (Exelis - Tysons Corner, VA) using 25 mm$\varnothing$ black (2%) and white (99%) diffuse reflectance standards (Labsphere inc. - North Sutton, NH). After calibration, the standard deviation of the reflectance at 600 nm was 0.26% and 0.34% on the black and white diffuse reflectance standards respectively. Image registration of the hyperspectral cubes of the same painting acquired before and after varnish removal was done using a novel point-based registration algorithm [21]; this algorithm achieves registration with a maximum error of 1/3 pixel.

#253141 Received 5 Nov 2015; revised 13 Dec 2015; accepted 14 Dec 2015; published 23 Dec 2015

Transmission measurements of the re-solubilized varnish were carried out with the FS3 spectroradiometer. Two 5 mm quartz cuvettes were prepared containing the pure solvent and the varnish solution respectively. The fiber collected the light reflected by the Spectralon white standard after passing through the pure solvent (white reference) and through the varnish solution (sample measurement). The transparency of the solvent (isopropyl alcohol for the impressionist panel, acetone for the still life) limited the spectral range from 350 to 1100 nm.

3. Description of light interaction with varnish/paint layer

To understand how the diffuse reflectance changes when an aged-varnish is removed and a new varnish is applied, reflectance measurements were carried out on 'Still Life' by Willem Kalf (Fig. 2). FORS measurements were made on the inner white portion of the delftware bowl. The measurements were made on the same spot and with the same collection geometry (Sec. 2) before and after aged varnish removal, and after a new varnish (MS2A working varnish) was applied. Comparison of the diffuse reflectance spectra before and after physical cleaning shows an increase in reflectance with the varnish removal over the entire spectral range measured (350 to 2500 nm) (Fig. 2). This increase can be described as the composite contribution of a constant (wavelength-independent) increase $\simeq 2.5\%$ in the whole range and a further increase in the visible range that gets gradually stronger (wavelength-dependent) approaching the UV/blue region. The wavelength-independent increase can be attributed in part to the uncovering of the rough paint surface. Two possible mechanisms can explain the wavelength-dependent increase in the visible: the first is the UV/blue absorption by the degradation products in the varnish. Another wavelength-dependent mechanism might arise from scattering phenomena: in fact, aged varnishes are known to have micro-cracks that contribute to a grayish haze. But the examination of the aged varnishes on test plates and on paintings suggests that the scale of the micro-cracks is too large to produce a wavelength-dependent scattering term. Nevertheless, these cracks may cause light being scattered and reflected by the aged varnish layer itself.

The application of a fresh varnish (MS2A) resulted in a wavelength-independent decrease in the measured diffuse reflectance $\simeq 1.2\%$ in the entire spectral range (Fig. 2). This is consistent with prior studies of the optical effect of varnishes and resins when applied to paintings [15]; namely the varnish reduces the painting roughness creating a new interface with air that is smoother than the air/paint interface.

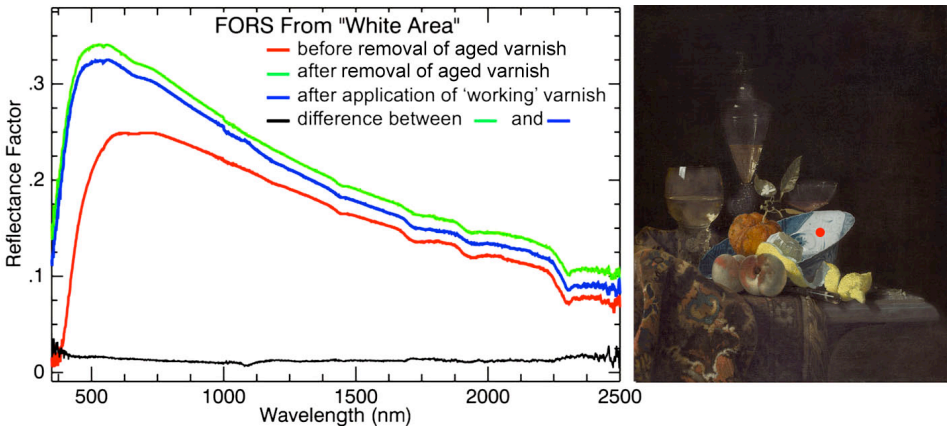

Fig. 2. "Still Life" by Willem Kalf, c. 1660 (National Gallery of Art, Washington DC - Chester Dale collection). The red spot in the color image of the painting (inside the delftware bowl) indicates where the multiple diffuse reflectance measurements were made.

#253141 Received 5 Nov 2015; revised 13 Dec 2015; accepted 14 Dec 2015; published 23 Dec 2015

These single point reflectance measurements offer a phenomenological model for the effects of aged varnishes on paintings. Following the literature [22,23], the radiation diffusely reflected by a paint surface (in the geometrical limit) can be separated into the reflection that occurs at the *interface* with air and the *body*-reflection (also called *volume*-). The first component, which takes place at the air/varnish interface of the varnished painting (or at the air/paint interface in the unvarnished case), is a wavelength-independent scattering term whose spectral distribution matches that of the incident radiation. The angular distribution of this interface scattering is dependent on the surface profile (i.e. roughness) of the illuminated area. The second component comes from the pigment/binder matrix, where the spectral distribution of the incident radiation is modified due to absorption and scattering by the binder embedded pigment particles.

4. Physical model for the light interaction with the varnish/painting system

In modeling the light interaction, some assumptions are made about the varnish/painting system (see Fig. 1). All pigment particles are immersed in the binding medium and the varnish wets the painting layer, so there is optical contact between binding medium and varnish. The varnish surfaces are optically smooth, while the exposed paint layer is rough. The fresh varnish is perfectly transparent (no absorption, no scattering), while the aged varnish shows discoloration and haze (blue absorption and body scattering).

The diffuse reflectances of the three different cases of Fig. 1 (aged varnish, no varnish, fresh varnish) include the contribution from multiple interface and body reflections.

The measured diffuse reflectance $R_{UC}(\lambda)$ of the uncleaned painting with aged varnish includes the reflection at the air/varnish interface (R_V^i), the body reflection of the varnish layer ($R_V^b(\lambda)$) and the body reflection of the painting ($R_P^b(\lambda)$) filtered in the double passage through the discolored varnish with transmittance $T(\lambda)$. The reflection at the interface between the paint and the varnish layer (old or new) is neglected because the difference between the optical indices of the paint binder and the varnishes is typically small (< 0.05) [15]. A high value of $R_V^b(\lambda)$ indicates a degraded varnish that has lost its transparency.

The measured diffuse reflectance $R_C(\lambda)$ of the cleaned, unvarnished painting is the sum of the reflection at the air/painting interface and the body reflection of the paint

$$R_C(\lambda) = R_P^i + R_P^b(\lambda). \tag{1}$$

The measured diffuse reflectance of the painting with the fresh varnish is constituted by the only body reflection of the paint ($R_P^b(\lambda)$).

The 'optical' removal of the aged varnish is described by an equation that relates $R_C(\lambda)$ to $R_{UC}(\lambda)$. A model that relates the diffuse body reflectances of a semi-transparent layer coating a substrate (ref. Fig. 1) is derived by Kubelka [24] from the two-flux approximation of the radiative transfer equation, which considers only two diffuse fluxes propagating perpendicular to the layer. The reflectance $R_{UC}(\lambda)$ of the varnished painting can be obtained from $R_P^b(\lambda)$, $T(\lambda)$ and R_V^b (the latter term being considered wavelength-independent -see Section 3) with the equation

$$R_{UC}(\lambda) = R_V^b + \frac{T^2(\lambda) R_P^b(\lambda)}{1 - R_V^b R_P^b(\lambda)}. \tag{2}$$

After algebraic rearrangement, the body reflectance of the clean painting is given by

$$R_P^b(\lambda) = \frac{R_{UC}(\lambda) - R_V^b}{T^2(\lambda) + R_V^b (R_{UC}(\lambda) - R_V^b)}. \tag{3}$$

#253141 Received 5 Nov 2015; revised 13 Dec 2015; accepted 14 Dec 2015; published 23 Dec 2015

Assuming varnish surfaces are optically smooth, their interface reflections are mostly specular and R_V^i can be neglected (since the specular component is excluded in the measurements); therefore the only interface reflection that is included in the measured diffuse reflectances is at the air/painting interface (R_P^i), which is indeed known to be rough. Combining Eqs.(1) and (3) the interface reflection is included, and $R_C(\lambda)$ is bounded to $R_{UC}(\lambda)$ by

$$R_C(\lambda) = \frac{R_{UC}(\lambda) - R_V^b}{T^2(\lambda) + R_V^b(R_{UC}(\lambda) - R_V^b)} + R_P^i. \tag{4}$$

The proposed procedure of virtual aged varnish removal is based on the physical model expressed by Eq. (4). The next section describes the method to measure/estimate the parameters.

5. Measurement/estimation of the parameters of the model

Diffuse reflectance from light and dark sites of the painting collected before and after local removal of the aged varnish ($R_{UC}^{white}(\lambda)$, $R_C^{white}(\lambda)$, $R_{UC}^{black}(\lambda)$, $R_C^{black}(\lambda)$) are measured.

Assuming the dark site as a black paint that is completely absorbing the incident radiation penetrating the interface ($R_P^b = 0$), a good estimation of R_V^b can be obtained by $R_{UC}^{black}(\lambda)$ [25], while R_P^i is estimated by $R_C^{black}(\lambda)$ (see Eq. (1)). Since R_V^b and R_P^i are assumed to be wavelength-independent, it is sufficient to have a strong absorption at a specific wavelength λ_0, so that

$$R_V^b = R_{UC}^{black}(\lambda_0) \qquad \textit{and} \qquad R_P^i = R_C^{black}(\lambda_0). \tag{5}$$

The other important actor in Eq. (4) is the transmittance of the varnish layer $T(\lambda)$, which can be determined from the diffuse reflectance measurements of the 'white' and the 'black' sites, combining Eq. (4) and Eqs. (5) in

$$T(\lambda) = \left[\frac{R_{UC}^{white}(\lambda) - R_{UC}^{black}(\lambda_0)}{R_C^{white}(\lambda) - R_C^{black}(\lambda_0)} - R_{UC}^{black}(\lambda_0)(R_{UC}^{white}(\lambda) - R_{UC}^{black}(\lambda_0)) \right]^{1/2}. \tag{6}$$

Thus all the variables in Eq. (4) are determined from the diffuse reflectance measurements.

As already discussed in the introduction, *black* appearing material accumulated over time can be found on the surface of paintings, as for instance candle soot or grease. This low-polarity material is not soluble in the polar solvent used by conservators, but yet it is mechanically removed together with the solubilized aged varnish during the mild chemical cleaning process.

Thus, the transmission resulting from Eq. (6) should be actually expanded in two terms, as

$$T(\lambda) = (1 - G)T_{varnish}(\lambda), \tag{7}$$

where the wavelength-independent factor G ($0 < G < 1$) accounts for the constant absorption of the "grime", while $T_{varnish}(\lambda)$ is associated with the aged varnish that absorbs primarily in the UV/blue region. A constant value of $T(\lambda)$ below 100% in the longer wavelengths (where the varnish does not absorb) can be mainly attributed to G, thus $T_{varnish}(\lambda)$ can be estimated.

While not necessary for virtual cleaning, it is phenomenologically interesting to verify that the removed aged varnish matches the estimated $T_{varnish}(\lambda)$. By soaking the soiled cotton swabs in the polar solvent used for cleaning, the removed aged varnish is re-solubilized and the transmittance of its solution can be measured ($T_{sol}(\lambda)$).

Given the phenomenological model advanced here, the following equality is expected to hold

$$T_{varnish}(\lambda) = T_{sol}(\lambda)^{\alpha} \tag{8}$$

with α being a factor that accounts for the different concentrations of the absorbing compounds in the layer on the painting and in the solution.

#253141 Received 5 Nov 2015; revised 13 Dec 2015; accepted 14 Dec 2015; published 23 Dec 2015

If the equality (8) is experimentally verified, the validity of the approach being presented is confirmed, and the light absorbed by the degradation products in the aged varnish can be considered the only acting wavelength-dependent phenomenon.

The next section reports the spectroscopic analysis of two paintings that underwent conservation treatment and the experimental verifications of Eq. (8).

6. Experimental measurements during actual aged varnish removal of two paintings

Two panel paintings with a large range of colors were measured repeatedly during the conservation treatment. The first is a small impressionist panel by Georges Seurat (in the following referred to as 'Haymakers') that had a thick yellow varnish. At the end of the conservation treatment the painting was left unvarnished, since Seurat despised that his paintings were varnished [26]. The lightest and the darkest sites of the painting were selected and FORS spectra were collected before and after small local cleanings. RIS was carried out before and after the complete removal of the aged varnish, and the hyperspectral cubes ($R_{UC}^{(x,y)}(\lambda)$ and $R_{C}^{(x,y)}(\lambda)$, with x and y expressing the location on the painting surface) were registered [21]. The values for the variables were provided with the procedure described in Section 5 using the diffuse reflectance spectra measured with FORS.

The second painting analyzed is a still life by Jan van Huysum (in the following referred to as 'Flowers') with a smoother and glossier paint surface, whose conservation treatment included the aged varnish removal and the final re-varnishing. RIS was carried out before and after the complete removal of the aged varnish, and a third time ($R_{IV}^{(x,y)}(\lambda)$) after the re-varnishing with a fresh resin (B-72), which acted as an isolation layer for the following inpainting. In order to simplify the procedure, the parameters of the model were taken from the reflectance spectra of the hyperspectral cubes by selecting the pixels corresponding to the lightest and the darkest sites of the painting. In this way the diffuse reflectance was measured with one instrument and one collection geometry only, resulting in a more homogeneous set of data.

Figure 3 shows a good verification of Eq. (8) opportunely adjusting the grime factor G and the exponent α (a part for a glitch below 420 nm in the curve of the 'Flowers' due to stray-light), confirming that the light absorbed by the degradation products in the varnish can be considered the only wavelength-dependent term to be included in the physical model.

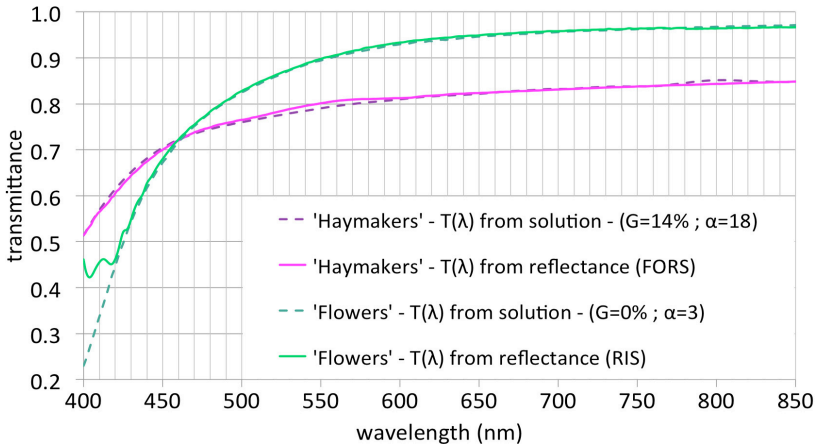

Fig. 3. In-situ single-pass transmission spectra of the aged varnish layer (including 'grime') calculated from the diffuse reflectance measurements (solid lines) and best fit scaled transmission of the re-solubilized varnish (dashed lines) for the two paintings examined.

#253141 Received 5 Nov 2015; revised 13 Dec 2015; accepted 14 Dec 2015; published 23 Dec 2015

The values of the variables are reported in Table 1 for the two paintings. A smaller interface reflection of the bare painting (R_P^i) was expected for the smoother and glossier surface of the 'Flowers' in comparison to the rougher 'Haymakers'. Figure 3 shows that the aged varnish absorption (including 'grime') of 'Haymakers' extended in the longer wavelengths ($T(\lambda) \simeq 85\%$ at 850 nm), indicating a high grime factor (14%) that is supported by the blackish material that remained on the cotton swabs used for cleaning. Cross-sectional microscopy revealed a layer of fine black particles embedded between two layers of varnish (data not shown). On the other hand, no unsolvable material was found to be accumulated on the 'Flowers' ($G = 0\%$).

Table 1. Values of the variables obtained in the experimental analysis.

	R_V^b	R_P^i	G	α
'Haymakers'	4.5%	6.1%	14%	18
'Flowers'	1.6%	1.9%	0%	3

7. Virtual cleaning: results & discussion

In view of the exposition in Section 4, virtual cleaning can be fulfilled by processing the hyperspectral cube collected before cleaning ($R_{UC}^{(x,y)}(\lambda)$) using

$$R_{VC}^{(x,y)}(\lambda) = \frac{R_{UC}^{(x,y)}(\lambda) - R_V^b}{T^2(\lambda) + R_V^b (R_{UC}^{(x,y)}(\lambda) - R_V^b)} + R_P^i. \tag{9}$$

$R_{VC}^{(x,y)}(\lambda)$ constitutes the prediction of the cleaned painting reflectances without varnish. The transmittance of the varnish layer $T(\lambda)$ (Fig. 3) and the scattering terms R_V^b and R_P^i (Table 1) were considered spatially invariant. Eq. (9) can also be used with a different scattering term for the paint to predict the reflectance after the application of a transparent fresh varnish.

Colorimetric calculations were carried out on the hyperspectral cubes to obtain the CIE XYZ tristimulus values, using the standard illuminant D65 and the 1964 supplementary standard colorimetric observer [7]. The coordinates in the CIELAB color space (whose perceptual uniformity is sufficient for our purposes) were calculated from the tristimulus values [27], and color differences were expressed with Euclidean distances ΔE.

Below 420 nm the hyperspectral camera showed some stray-light, which was often emphasized by the mathematical manipulation, as for instance is the case of the transmittance calculated from the RIS spectra of the 'Flowers' (Fig. 3 - green solid line). For this reason, the wavelengths below 420 nm have been excluded from the colorimetric calculations. The ΔE associated with the exclusion of this spectral range has an average of 0.6 for the 'Haymakers' and 0.9 for the 'Flowers'. At the expense of this imperceptible color inaccuracy, the contribution of potential artifacts in the results due to stray-light has been avoided. The results expressed in terms of colorimetric difference that are presented at the end of this paper would change by two decimal or less if the spectral range was not restricted (data not shown).

7.1. 'Haymakers at Montfermeil'

The study of the 'Haymakers' started when $1/3$ of the painting surface had already been physically cleaned, i.e. aged varnish and grime removed. Reflectance Imaging Spectroscopy (RIS) was carried out before and after the physical cleaning of the remaining $2/3$. The $1/3$ of the painting that had already been cleaned offered the opportunity to determine the repeatability of RIS measurements, acting as a 'control region'. In this control region (the red rectangle in figure 4 - top-right) the average ΔE determined from the RIS measurements before ($R_{UC}^{(x,y)}(\lambda)$)

#253141 Received 5 Nov 2015; revised 13 Dec 2015; accepted 14 Dec 2015; published 23 Dec 2015

and after ($R_C^{(x,y)}(\lambda)$) physical cleaning was 1.8 with a standard deviation of 0.6. These values are around the threshold of perceptible color difference and indicate a satisfactory repeatability of the hyperspectral measurement.

The ΔE between the colorimetric values before and after physical cleaning of the area outside the control region is a measure of how much the aged varnish and the grime affected the painting color appearance. The average ΔE in this area (the cyan rectangle in Fig. 4 - top-right), was 8.3 with a standard deviation of 2.0, indicating a large perceivable color change.

The image on the bottom-right of Fig. 4 contains the ΔE between the colorimetric values after actual and virtual cleaning, which represents a metric for the degree of success of the virtual cleaning. Since the model was used to process the complete image, the control zone was of no interest in this case (masked out with red stripes). The average ΔE inside the green rectangle in Fig. 4 (bottom-right) was 3.1, with a standard deviation of 1.5. Even if this residual colorimetric distance is slightly perceptible by eye, it is not far from the experimental error (1.8) indicating that the virtual cleaning was quite effective.

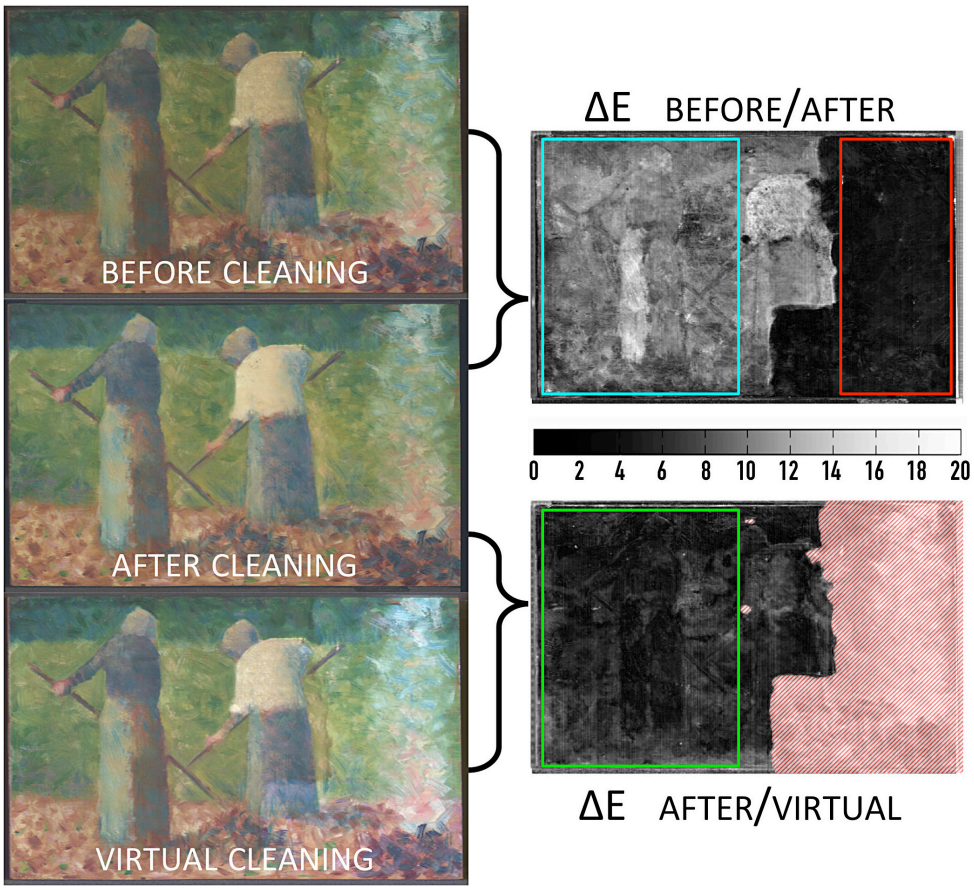

Fig. 4. G. Seurat, 'Haymakers at Montfermeil', c. 1882 (National Gallery of Art, Washington DC - Collection of Mr. and Mrs. Paul Mellon). Left: color images of painting before (top) and after physical removal of aged varnish (center), and predicted appearance with virtual cleaning (bottom). Right: ΔE between the images before and after actual cleaning (top) and between the images after actual and virtual cleaning (bottom). The 1/3 on the right of the painting had already been cleaned and acted as a 'control region'.

#253141 Received 5 Nov 2015; revised 13 Dec 2015; accepted 14 Dec 2015; published 23 Dec 2015

7.2. *'Flowers in an urn'*

The experimental study of the 'Flowers' was focused on the central part of the painting where the large range of saturated colors is concentrated. The average ΔE across the analyzed region before and after actual varnish removal (i.e. the color change due to the treatment that left the painting unvarnished) was 10.7 with a standard deviation of 4.7.

After virtual cleaning the residual average ΔE was 4.2 with a standard deviation of 1.9, indicating a perceivable color difference between the predicted and measured images of the painting without varnish. To investigate the cause of this residual discrepancy, the reflectance spectra from the hyperspectral cubes were analyzed for some selected spots of the painting. In areas of low ΔE the curves show a good match between the predicted $R_{VC}(\lambda)$ and the measured reflectance $R_C(\lambda)$ after varnish removal, as for instance is the case for the light blue, red, pink and white points reported in the top part of Fig. 5. However, other points of the painting did not show the same good prediction and the ΔE is consequently high, as for instance is the case for the two points reported in the bottom of Fig. 5. The spectra of the green point (Fig. 5 - left) indicate that the optical density of the aged varnish layer was higher in that specific point, as

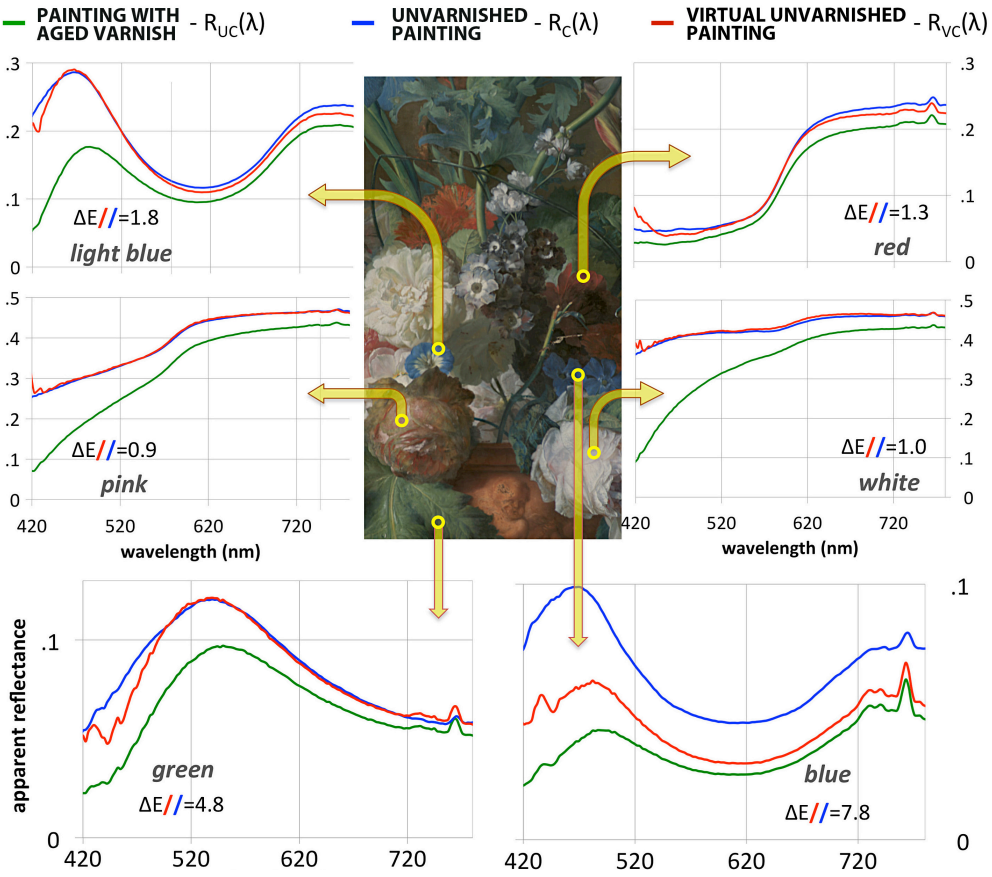

Fig. 5. Detail of 'Flowers in an urn' by J. Van Huysum, c. 1721 (National Gallery of Art, Washington DC - Adolph Caspar Miller Fund). Color image of the cleaned, unvarnished painting and reflectance spectra measured with RIS before and after varnish removal ($R_{UC}(\lambda)$ and $R_C(\lambda)$) and the reflectance predicted with virtual cleaning ($R_{VC}(\lambda)$) for six selected points.

#253141 Received 5 Nov 2015; revised 13 Dec 2015; accepted 14 Dec 2015; published 23 Dec 2015

the predicted and measured curves diverge below 500 nm (the region where varnish absorption is stronger). On the other hand, the large offset between the predicted and measured reflectance spectra of the blue point (Fig. 5 - right) can be interpreted as an underestimation of R^i_P.

This spatial variability in varnish transmission and painting roughness, which was found to be stronger for the 'Flowers', suggests that a procedure that assumes constant parameters across the painting is not always effective. Actually, the type of pigment and the size of its particle influence the surface roughness of the paint layers. As a consequence, the air/painting interface scattering R^i_P may vary considerably across the painting following the distribution of the pigments. A layer of fresh varnish, besides making the painting smoother, makes the residual roughness more homogeneous, and this should result in an interface scattering with a lower spatial variability.

The virtual cleaning of the 'Flowers' was performed a second time (VC^*) with the aim to match the appearance of the painting after the isolation varnishing prior to inpainting ($R^{(x,y)}_{IV}(\lambda)$). The thin layer of B-72 was considered transparent ($T(\lambda) = 1$ in the entire spectral range), creating a surface with a residual roughness; in fact, thin varnish layers partly reproduce the roughness of the underlying paint [15], especially varnishing with B-72 that does not level the surface roughness as for instance mastic or Regalrez® [16]. The new scattering term, estimated from the reflectance of the selected dark point of the painting, was $R^i_{IV} = 1.6\%$. The physical model (Eq. (9) was applied with R^i_{IV} in place of R^i_P and the colorimetric result is reported in Fig. 6. The residual average ΔE after virtual cleaning was 3.8, with a standard de-viation of 1.6 (the red points in the ΔE image of Fig. 6 correspond to removed old inpaintings that were not included in the calculation of the mean).

Fig. 6. Detail of 'Flowers in an urn' by J. Van Huysum, c. 1721 (National Gallery of Art, Washington DC - Adolph Caspar Miller Fund). From left: color images of the painting with the aged varnish (1), after removal of the aged varnish and fresh varnishing (2), and after virtual cleaning aiming to match the freshly varnished painting (3). On the right:ΔE between the predicted and measured colorimetric values - the areas highlighted in red correspond to old inpaintings that were removed during the treatment.

Table 2 recapitulates for the two paintings the colorimetric results of virtual cleaning expressed as initial and residual average ΔE.

#253141 Received 5 Nov 2015; revised 13 Dec 2015; accepted 14 Dec 2015; published 23 Dec 2015

Table 2. Color change with treatment and results of virtual cleaning predicting the appearance of the painting after physical varnish removal (first two rows) and after application of a new varnish (last two rows). The experimental error is ΔE=1.8.

	'Haymakers'	'Flowers'
ΔE between $R_{UC}^{(x,y)}(\lambda)$ and $R_{C}^{(x,y)}(\lambda)$ color change with varnish removal	mean = 8.3 st dev = 2.0	mean = 10.7 st dev = 4.7
ΔE between $R_{VC}^{(x,y)}(\lambda)$ and $R_{C}^{(x,y)}(\lambda)$ residual color difference after virtual cleaning	mean = 3.1 st dev = 1.5	mean = 4.2 st dev = 1.9
ΔE between $R_{UC}^{(x,y)}(\lambda)$ and $R_{IV}^{(x,y)}(\lambda)$ color change with varnish removal and new varnishing	*not re-varnished*	mean = 9.5 st dev = 5.0
ΔE between $R_{VC^*}^{(x,y)}(\lambda)$ and $R_{IV}^{(x,y)}(\lambda)$ residual color difference after virtual cleaning	*not re-varnished*	mean = 3.8 st dev = 1.6

8. Conclusion

This work presented a phenomenological and physical model that describes the alteration of the spectral reflectance of paintings due to the presence of an aged varnish. The experiential data show that virtual cleaning - i.e. aged varnish removal through hyperspectral image processing - requires modeling the aged varnish with a transmission function and including scattering terms. This has been shown by examining a small painting by Georges Seurat and a still life by Jan van Huysum, both followed during their conservation treatment. The colorimetric results of virtual cleaning are satisfactory, showing that the presented model is able to positively predict the reflectance of the cleaned painting with a few point-based diffuse reflectance measurements before and after local varnish removal with solvents.

The physical model has been also applied to FORS measurements from 'Venus with a mirror' by Titian, which had a strongly discolored varnish. The reflectance after the aged varnish removal was predicted using the transmission spectrum of the re-solubilized varnish. A 15th century panel by an unknown Tuscan artist and 'Field with irises near Arles' by Vincent Van Gogh were imaged with RIS and the physical model was used to process the process the hyperspectral cubes, providing convincing images of the paintings after cleaning.

The discrepancies shown in this paper as images of residual colorimetric differences are ascribable to spatial variations in the characteristics of the aged varnish (optical density, scattering properties) and the underlying painting (roughness).

These observations outline new possibilities to model spatially varying roughness of paint layers, contributing to create more realistic reproductions of works of art through 3-D printing.

Acknowledgments

The authors wish to thank the conservators Dina Anchin, Ann Hoenigswald and Kirstin deGhetaldi, who treated the paintings. Michael Palmer for the analysis of the cross-sections. Andrea Casini for his technical support. The advice from Barbara Berrie, Kathryn Dooley and Melanie Gifford. The authors acknowledge financial support from the Andrew W. Mellon and Samuel H. Kress Foundations, and from the National Science Foundation (award n.1041827). E. René de la Rie participated in the early stages of the research. This work leverages many of his pioneering studies in the field of varnish research in art conservation.

#253141 Received 5 Nov 2015; revised 13 Dec 2015; accepted 14 Dec 2015; published 23 Dec 2015